

# Performance Testing of a High Effectiveness Recuperator for High Capacity Turbo-Brayton Cryocoolers

**D. Deserranno<sup>1</sup>, M. Zagarola<sup>1</sup>, D. Craig<sup>2</sup>, R. Garehan<sup>2</sup>, T. Giglio<sup>2</sup>,  
J. Smith<sup>2</sup>, J. Sanders<sup>3</sup>, M. Day<sup>3</sup>**

<sup>1</sup>Creare, Hanover, NH 03755, USA

<sup>2</sup>Mezzo Technologies, Baton Rouge, LA 70814, USA

<sup>3</sup>Edare, Lebanon, NH 03766, USA

## ABSTRACT

NASA is considering multiple missions involving long-term cryogen storage in space. Liquid hydrogen and liquid oxygen are the typical cryogens as they provide the highest specific impulse for chemical propellants. The net heat load to a hydrogen tank storing 38 metric tons of liquid hydrogen is estimated to be 20 W at 20 K. To enable long-duration zero boil-off storage, this heat load must be lifted using an active refrigerator. Creare is addressing this need by developing a turbo-Brayton cryocooler that provides 20 W of refrigeration at 20 K.

The key components in the 20 K, 20 W cryocooler are the electronics, compressors, turboalternator, and recuperators. The recuperator for the 20 K, 20 W cryocooler is a five-module micro-shell-and-tube heat exchanger developed jointly by Creare, Mezzo Technologies and Edare. It has a predicted effectiveness exceeding 0.995, enabling the cryocooler to deliver 20 W of refrigeration for an input power around 1.6 kW, corresponding to a specific power of about 80 W/W. This is significantly better performance than any 20 K cryocooler existing or (to our knowledge) under development. In preparation of the cryocooler integration, a recuperator module was tested between 300 K and 20 K using helium at design flow rates. The test results indicated the recuperator exceeded its target effectiveness.

## INTRODUCTION

NASA is evaluating long-term liquid hydrogen and oxygen storage in low Earth orbit to support the chemical propulsion needs of future missions. Researchers at NASA investigated a co-storage concept for these cryogenic propellants [1]. Here the liquid oxygen tank at 90 K intercepts a large fraction of the heat load to the hydrogen tank at 20 K. The shielding provided by the oxygen tank can be augmented using an actively cooled shield. As a result, the radiative heat flux to the hydrogen tank reduces from 0.25 W/m<sup>2</sup> to 0.02 W/m<sup>2</sup>. The net heat load to a hydrogen tank storing 38 metric tons of liquid hydrogen is estimated to be 20 W at 20 K, including design margin. To enable long-duration zero boil-off storage, this heat load must be lifted using an active refrigerator. Unfortunately, this heat load exceeds the capacity for any space cryocooler demonstrated to date.

Creare is addressing this shortcoming by developing for NASA a turbo-Brayton cryocooler that provides 20 W of refrigeration at 20 K [2]. Turbo-Brayton cryocoolers are ideal for long-term liquid

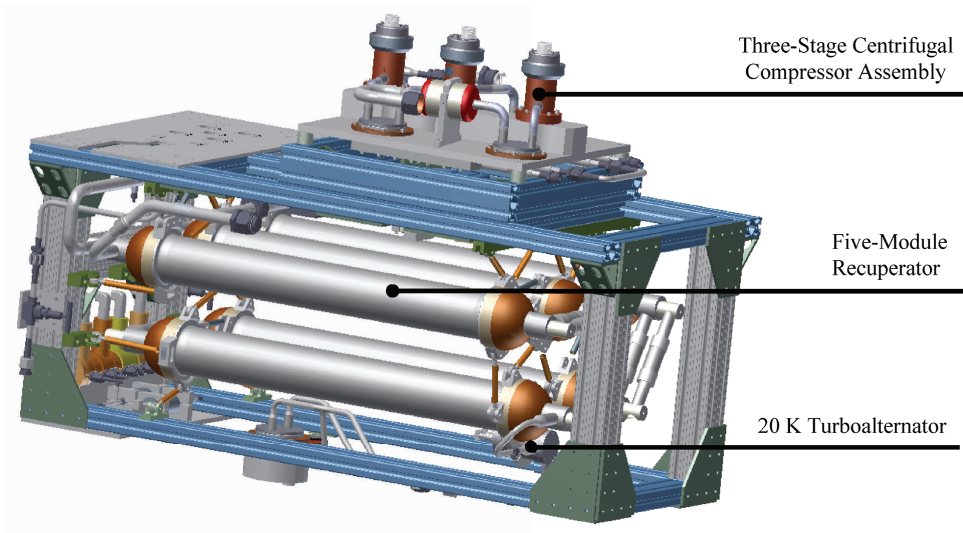


**Figure 1.** Creare's 20 K, 20 W cryocooler for liquid hydrogen storage.

hydrogen storage in space because of favorable mass and performance scaling to high capacities and low temperatures. In addition, the continuous flow nature of the cycle provides a means to directly interface with a Broad Area Cooling (BAC) system attached to the hydrogen tank without the mass and performance penalties associated with ancillary cryogenic heat pipes or circulation loops. The cryocooler designed for this application is shown in Figure 1. It delivers 20 W of cooling at 20 K for an input power around 1.6 kW, corresponding to a specific power of 80 W/W. The coefficient of performance of the cryocooler is 18% of the Carnot cycle. This is significantly better performance than any 20 K cryocooler existing [3] or (to our knowledge) under development.

The key mechanical components in the 20 K, 20 W cryocooler are the compressors, turboalternator, and recuperators. The compressors [4] and turboalternators [5] have been previously demonstrated at the required capacity and only minor modifications are required for use in the 20 K, 20 W cryocooler. While many recuperators have been space qualified, none have the capacity required for a 20 K 20 W cryocooler. Indeed, most turbo-Brayton cryocoolers operating near or below 20 K have a capacity below 1 W [6]. As a result, an order of magnitude increase in the cryocooler and recuperator capacity is required. Unfortunately, using many lower capacity recuperators in parallel leads to significant packaging, costs, and flow distribution concerns. A new type of recuperator is required for high capacity turbo-Brayton cryocoolers. The design, fabrication, and testing of a high capacity recuperator is the subject of this paper.

## SIGNIFICANCE AND JUSTIFICATION FOR DEVELOPMENT

After an initial trade study, Creare pursued the development of a micro shell-and-tube heat exchanger to serve as the recuperator in the 20 K, 20 W cryocooler and enlisted a development team comprising Creare, Mezzo Technologies, and Edare. While conventional shell-and-tube heat exchangers are common in industry, their mass is prohibitive for space applications due to the large size tubes. The use of micro-tubes allows for significant mass savings, as a large amount of area can be packaged within a small volume. Given prior experience at Mezzo Technologies, the development team opted to pursue a unit using 0.022 inch diameter micro-tubing. The primary technical challenge is to fabricate this unit with 100% hermetic joints between the high and low pressure streams.

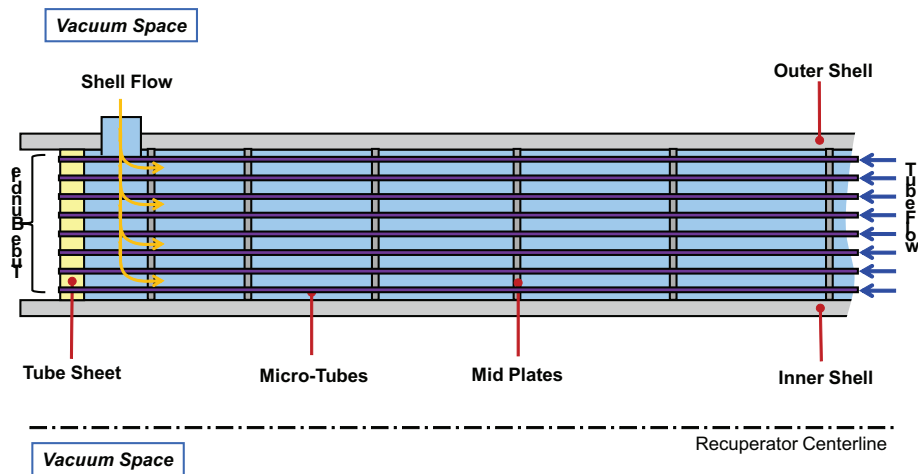


Figure 2. High capacity recuperator schematic.

RECUPERATOR DESIGN AND ANALYSIS

A recuperator was designed based on the requirements of the cryocooler, resulting in the need for over 6,600 micro-tubes having an outer diameter of 0.022 inch, each over 150 inches long. Due to the excessive length, the recuperator was divided into 5 serial modules for ease of fabrication and packaging. Each module is nominally 40 inches long, including its headers. The heat transfer zone within the module is 30 inches long. The cross section of the core is annular in nature with an inner diameter of 2 inches and an outer diameter of 4 inches (illustrated in Figure 2). Various thermal-fluid analyses were performed using computational fluid dynamics to assess the performance of the micro-tube heat exchanger and the impact of various design features on flow distribution within the core. The core overall effectiveness is assessed taking into account local flow maldistribution effects, resulting in regions of local flow capacitance imbalance. The nominal operating conditions of the recuperator are 3.6 g/s of helium; tube-side inlet pressure of 7.9 atm and inlet temperature of 300 K, and shell-side inlet pressure of 5.6 atm and inlet temperature of 20 K.

The predicted recuperator loss of the five-module recuperator is 17.7 W, including parasitics. The recuperator loss is defined as the cold-end stream-to-stream enthalpy difference multiplied by the recuperator mass flow rate. This loss must be absorbed by the turboalternator of the cryocooler, in addition to the cryocooler heat load. The parasitics depend highly on the packaging and configuration of the cryocooler. For the configuration shown in Figure 1, the recuperator assembly is mounted to a 300 K platform and the conductive and radiative parasitics are predicted to be 5.8 W. The thermal performance of the individual modules (including conductive and radiative parasitics) is shown in Table 1. The variation in the log mean temperature difference is the result of real-gas effects of helium near 20 K and thermal parasitic. The decrease in module UA (conductance) as

Table 1. Predicted recuperator module performance with parasitic losses.

	Mod 1	Mod 2	Mod 3	Mod 4	Mod 5
Warm Temperature (K)	300.0	248.7	203.4	146.1	80.4
Cold Temperature (K)	248.4	203.0	145.6	79.7	20.0
Minimum Stream Capacity (W/K)	18.6	18.6	18.6	18.6	18.9
Log Mean Temperature Difference (K)	0.235	0.258	0.372	0.525	0.748
UA (W/K)	4082	3310	2905	2364	1521
Total Heat Transfer (W)	960	854	1081	1242	1138
Effectiveness	0.987	0.992	0.993	0.992	0.989

the recuperator temperature decreases is the result of decreasing gas thermal conductivity which decreases the heat transfer coefficient.

In addition to thermal-fluid analyses, structural analyses were conducted to assess the mechanical performance of the unit in a launch environment. Specifically, the recuperator was designed to meet the requirement of NASA’s General Environmental Verification Standard (GEVS), as described in NASA TM GSFC-STD-7000A, a standardized set of environmental exposure standards for payloads, subsystems, and components. The analyses performed were (1) a hydrostatic pressure analysis and (2) a random vibration analysis. Pressure stresses were computed for a 16 atm maximum design pressure (MDP). Analysis was performed at MDP and stresses were compared against allowable values per ASME B31.3 (incorporating proof pressure conditions and design margins). Random vibration analysis was performed consistent with GEVS random vibration test levels for a 90 kg system based on the expected mass of the cryocooler. The random vibration analysis assumed a 1% dampening ratio ( $Q=50$ ). The recuperators exhibited margin relative to the yield stress under all analysis conditions.

**RECUPERATOR FABRICATION**

The key step in the fabrication of the heat exchanger is the joining of the micro-tubes to the tubesheets. Based on analysis, it can be shown that significant performance degradation can be caused by even a few non-hermetic joints between the high and low pressure stream. For this specific design, a 99.8% weld joint reliability is required to ensure the cryocooler delivered 95% of its design cooling capacity. Laser welding was pursued to join the micro-tubes to the tubesheets. The primary advantage of laser welding is the ability to repair joints, allowing the fabrication of 100% hermetic recuperators.

The weld reliability of each joint is dependent on the laser settings as well as the geometric features of the joint. Therefore, laser welding process parameters were developed through an iterative process. Sectioning of weld joints was performed in small sample sets to identify potentially suitable conditions. Once reasonable geometric features and laser parameters were established, a reliability study was performed by welding thousands of joints with the desired settings. An iterative process was used until the resulting weld joint reliability was sufficiently high (>99.8%) such that repair options were practical.

To aid the welding process, off-axis cameras were installed to enable real-time pre- and post-inspection of the weld joint (Figure 3). This allows for the inspection of critical weld joint features such as the protrusion of the micro-tube above the tubesheets prior to completing the welding process. Furthermore, a visual inspection of the completed joint allows for the real-time identification of leaky joints. An example of pre- and post-welding images is shown in Figure 3. In the pre-weld condition, we can visualize the alignment of the laser and the weld joint (left image) and the pro-

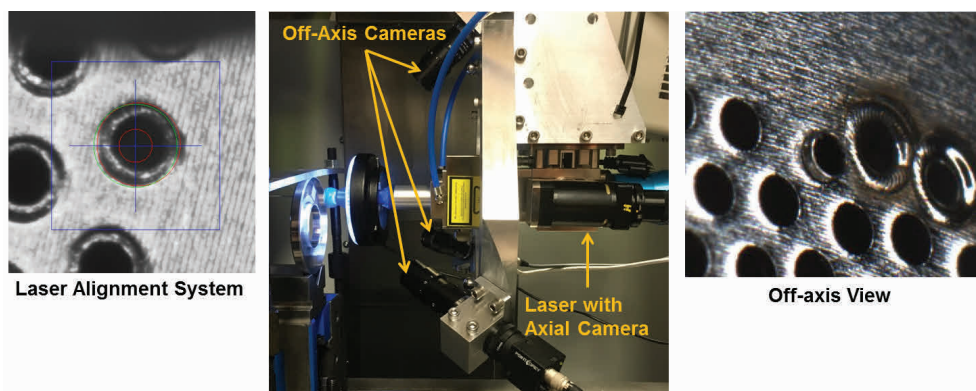


**Figure 3.** Micro-tube laser welding system.

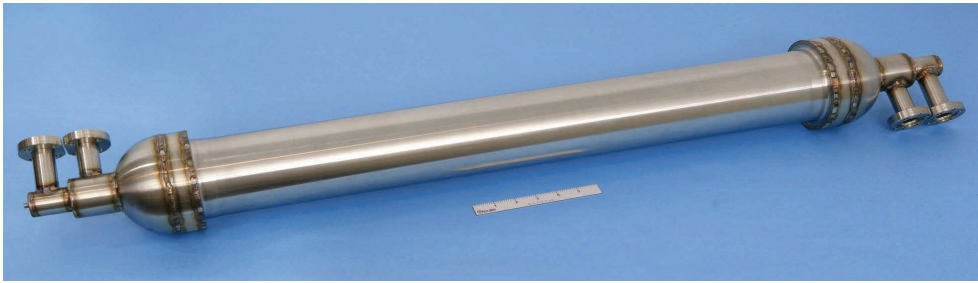


**Figure 4.** Completed recuperator following proof-pressure testing.

trusion of the tube above the tubesheet (right image). In the post-weld condition, we can see the completed weld joint, allowing us to identify potential flaws in the joint.

When both tubesheets are welded, a bubble-point leak check is performed to identify non-hermetic joints. These joints are subsequently repaired until a fully hermetic unit is obtained. Headers are then welded to the recuperator core, and the unit is proof-pressure tested based on the requirements of the cryocooler. The completed recuperator module is shown in Figure 4. Following fabrication, a variety of workmanship screening tests are performed, including external leak check, cross-stream leak check, and pressure versus flow tests. The unit passed all tests.

**RECUPERATOR THERMAL TESTING**

The recuperator was tested under cryogenic conditions to evaluate its thermal effectiveness. While the expected operation of each recuperator module spans a smaller temperature range, the resulting stream-to-stream temperature difference is too small to ensure adequate fidelity in our test due to measurement uncertainty. Therefore, the stream-to-stream temperature difference is artificially increased to allow us to more reliably characterize the recuperator performance. To accomplish this, the warm end of the recuperator was held at room temperature, while the cold end was operated between 20 K and 50 K. The test facility schematic is shown in Figure 5. Temperatures are measured at the inlets and outlets of the recuperator using redundant, in-line Platinum Resistance Thermometers (PRTs), and the flow rate is measured using a spring-loaded rotameter. The facility

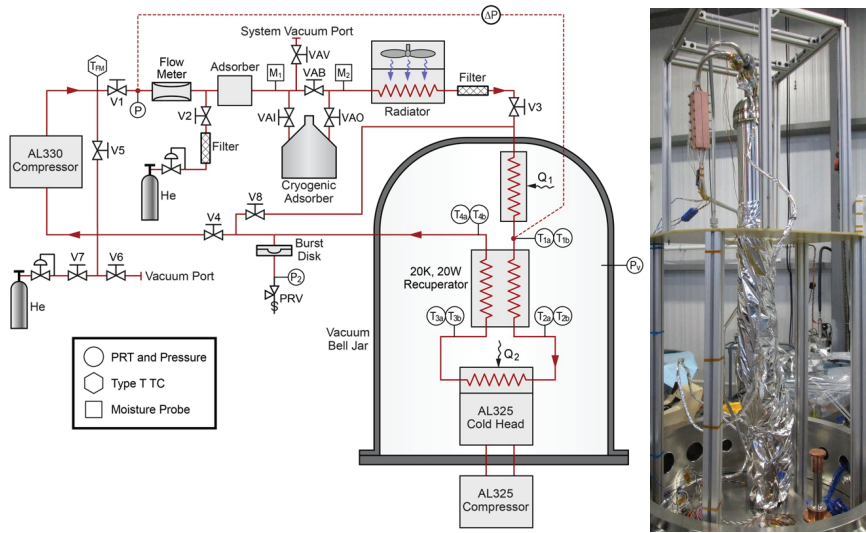


**Figure 5.** Cryogenic thermal test facility system.



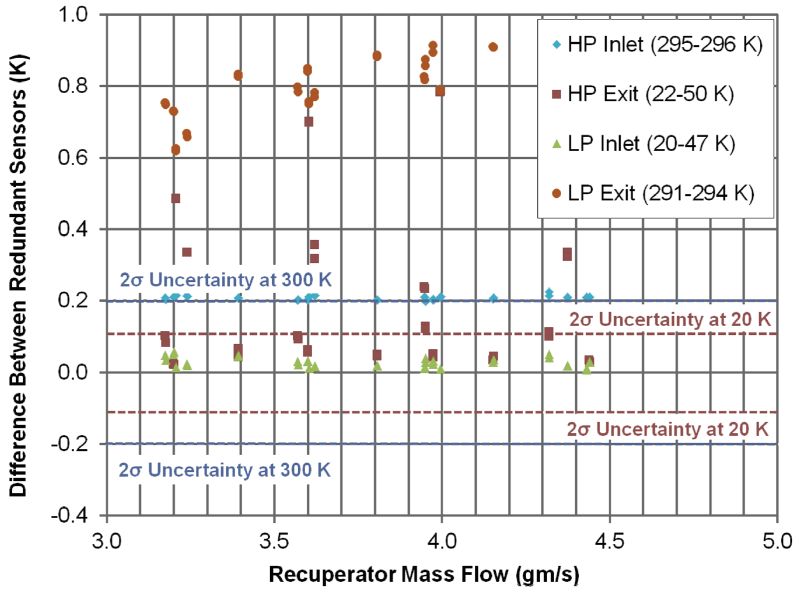


**Figure 6.** Agreement between redundant temperature sensors.

operates as a closed-loop, allowing us to test for extended time periods. The recuperator is covered with Multi-Layer Insulation (MLI; 20 layers at the cold end and 3 layers at the warm end) to limit parasitic losses to below 1 W, which is a small fraction of the total heat transfer rate within the unit (nominally 5 kW). Based on the instrumentation accuracy, the anticipated errors are  $\pm 3\%$  for the ineffectiveness, and  $\pm 4\%$  for the UA product.

A total of 19 steady-state test points were collected for a nominal warm temperature of 295 K, and a cold temperature ranging from 20 K to 50 K. The heat transfer between the two streams varied between 4.2 kW and 6.2 kW, depending on the test conditions. The heat imbalance between the two streams averaged 6.0 W or 0.11%, and was within the accuracy of the sensors. Figure 6 illustrates the agreement between the redundant temperature sensors at the inlets and exits of the recuperator. The inlet sensors have a strong agreement (within the  $2\sigma$  uncertainty band) at both the warm and cold end of the recuperator. This is to be expected due to the temperature uniformity in the incoming flow. The exit sensors demonstrate some level of disagreement, likely due to stratification in the exit flow as a result of minor flow maldistribution effects.

The thermal ineffectiveness results are shown in Figure 7 as a function of mass flow rate. Throughout the development of the recuperator technology, various iterations were performed on the design and assembly process. As illustrated in Figure 7, each iteration significantly reduced thermal ineffectiveness. Ultimately, our first production unit achieved the single module target ineffectiveness of 1.2% at the design flow rate of 3.6 g/s. Ineffectiveness has a weak correlation to the recuperator cold-end temperature, but strongly correlates with the mass flow rate through the unit. As flow rate is increased, the ineffectiveness increases slightly as demonstrated by our test data and predictions.

## RECUPERATOR VIBRATION TESTING

In addition to thermal performance testing, a recuperator module was vibrated in both the axial direction and one transverse direction (Figure 8). Due to symmetry of the recuperator and the fixturing, no testing was done in third direction. The recuperator was tested with the NASA GEVS spectrum, modified for a system mass of 90 kg. Testing was performed at +3 dB, 0 dB, and +3 dB relative to this spectrum. The 3 dB, 0 dB, and +3dB tests corresponds to 5.2 Grms, 7.4 Grms, and

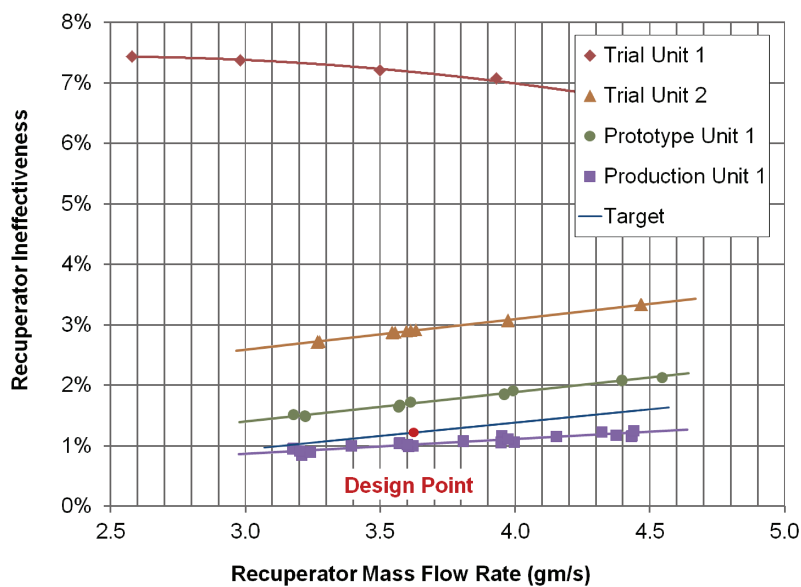


Figure 7. Thermal ineffectiveness of the recuperators throughout the development process.

10.4 Grms, respectively. Due to shaker table limitations, the +3 dB test was limited to 9 Grms. Using the modified GEVS spectrum, the following profiles were applied:

- 1. Axial direction, 3 dB below specification, for 3 minutes
- 2. Axial direction, at specification, for 3 minutes
- 3. Axial direction, at specification, for 27 minutes
- 4. Axial direction, 3 dB above specification, for 3 minutes
- 5. Lateral direction, 3 dB below specification, for 3 minutes
- 6. Lateral direction, at specification, for 3 minutes
- 7. Lateral direction, at specification, for 27 minutes



Figure 8. Vibration test configuration for the transverse tests on the prototype unit.

The 27-minute tests are substantially longer than those required by GEVS, and were accidental. Prior to testing, characterization tests were performed to determine the damping. The damping was found from the width of the response curve at the half power points. The measured quality factor in the lateral direction was  $Q=18$  at 160 Hz resonant frequency, and in the axial direction was  $Q=28$  at 135 Hz resonant frequency. The quality factor was considerably less than assumed in the analysis ( $Q=50$ ), so notching at the resonant frequencies was not required. Before and after each vibration test, a 0.5 G sinusoidal sweep, external leakage, and cross-stream leakage tests were performed to assess recuperator failure. The recuperator module passed all random vibration testing including the extended duration testing.

## CONCLUSIONS

Creare, in collaboration with Mezzo Technologies and Edare, developed a lightweight, high-capacity, high-effectiveness recuperator technology, suitable for use in space missions. This paper discussed the design, fabrication, and testing of the recuperator. A 5-module recuperator has a predicted effectiveness exceeding 0.995, enabling a 20 K cryocooler to deliver 20 W of refrigeration for an input power around 1.6 kW, corresponding to a specific power of about 80 W/W. In addition to thermal performance testing, a unit was vibration tested successfully under space launch conditions. Future work involves building the remaining recuperator modules, integrating them into a cryocoolers, and testing the cryocooler.

## ACKNOWLEDGMENT

We gratefully acknowledge NASA for their support of this work (Contracts NNX13CL57P and NNC14CA15C).

## REFERENCES

1. Mustafi, S., Canavan, E.R., and Boyle, R., "Co-Storage of Cryogenic Propellants for Lunar Exploration," *AIAA 2008-7800*, AIAA SPACE 2008 Conf & Expo, San Diego, CA (2008).
2. Deserranno, D., Zagarola, M.V., Li, X. and Mustafi, S., "Optimization of a Brayton Cryocooler for ZBO Liquid Hydrogen Storage in Space," *Cryogenics*, vol. 64, (2014), pp. 172–181.
3. Cha, J.S. and Yuan, S.W., "Space Cryocooler Vendor Survey Update: 2013," Aerospace Report TOR-2013(3905)-4, The Aerospace Corporation, El Segundo, CA (2013).
4. Hill, R.W., Hilderbrand, J.K. and Zagarola, M.V., "An Advanced Compressor for TurboBrayton Cryocoolers," *Cryocoolers 16*, ICC Press, Boulder, CO (2011),
5. Zagarola, M.V., Cragin, K.J. and Deserranno, D., "Demonstration of a High-Capacity Turboalternator for a 20 K, 20 W Space-Borne Brayton Cryocooler," *Adv. in Cryogenic Engineering*, Vol. 59, Amer. Institute of Physics, Melville, NY (2014), pp. 1432–1437.
6. Breedlove, J.J., Cragin, K.J. and Zagarola, M.V., "Testing of a Two-Stage 10 K Turbo-Brayton Cryocooler for Space Applications," *Cryocoolers 18*, ICC Press, Boulder, CO (2015),